Article

Journal of Vibration and Control
2016, Vol. 22(6) 1593–1603

DOI: 10.1177/1077546314543730
jvc.sagepub.com

Solutions of dynamic and acoustic responses of a clamped rectangular plate in thermal environments

Qian Geng and Yueming Li

Abstract

This work presents an investigation of vibration and acoustic response characters of a clamped rectangular thin plate in thermal environments. The general form of governing equation of plate flexural vibration with considering thermal loads is established, and the influence of uniform temperature change on response characters is studied in detail. A set of double sinusoidal mode shape functions for fully clamped boundaries is used to describe the displacement distribution. The governing equation is solved with Fourier series expansion to discuss the natural vibration and dynamic responses of a clamped plate in thermal environments. Accordingly, acoustic radiation characteristics are obtained based on Rayleigh integral. Results show that natural frequencies decrease with the increment of plate temperature, and the first natural frequency is much more sensitive to thermal environment changes. Response curves of plate vibration and radiated sound power shift toward lower frequency range, and the response amplitudes of the first resonant peak of the two responses present opposite variation tendencies. These phenomena are verified with finite element and boundary element simulations. Thermal loads reduce the radiation efficiency of the plate obviously below the critical frequency, but the maximum value almost remains unchanged.

Keywords

Thermally stressed vibration, governing equation, Fourier series solution, acoustic radiation, FE-BE simulation

1. Introduction

In space explorations, vehicles usually work in many different environments, which will generate kinds of applied loads or change the state of structures. With the increment of flight speed, thermal environment has become an important influence factor to vehicles due to serious aerodynamic heating (Behrens and Muller, 2004). The performance of structures in thermal environments has become a hot topic.

Research on thermo-vibration of structures can date back to about middle of the 20^{th} century (Boley, 1956; Boley and Barber, 1957). As elementary structures, plates have been widely studied. Jadeja and Loo (1974) investigated thermally induced dynamic behavior of a rectangular plate subjected to a sinusoidal heat flux. An approximate solution with double trigonometric series was used to solve the problem. They found that the inertia terms are very important for heated plates during dynamic procedures. Ganesan and Dhotarad (1984) studied the vibration responses of thermally stressed plates with numerical methods. Finite element method (FEM) was used in thermostatic analysis to obtain thermal stresses, and finite difference technique and variational approach were applied in the subsequent dynamic analysis. Yeh (2005) investigated the vibration of a simply supported orthotropic plate with large deflection considering the coupled thermo-mechanical effect. The results indicated that the coupling effect acts as a thermo-elastic damping which causes a decay of the vibration amplitude. The coupled thermo-mechanical effect should be considered when the initial deflection of plates is large.

State Key Laboratory for Strength and Vibration of Mechanical Structures, Xi'an Jiaotong University, China

Received: 27 January 2014; accepted: 26 May 2014

Corresponding author:
Yueming Li, State Key Laboratory for Strength and Vibration of Mechanical Structures, Xi'an Jiaotong University, No. 28 Xianning West Road, Xi'an, 710049, China.
Email: liyueming@mail.xjtu.edu.cn

Kim (2005) developed an analytical method to study the vibration behavior of functionally graded rectangular plates in thermal environments. Thermal stresses and temperature dependent material properties were considered in the study. Results confirmed that material compositions, plate geometry and temperature variation would influence the dynamic responses significantly.

Along with the vibration procedure, structures radiate sound simultaneously. This would affect the ambient environment and might be harmful to the facilities and human beings (Wilby, 1996). Studies of acoustic radiation characters of vibrating plates have been carried out along with the investigations of dynamic behavior of structures (George, 1961; David, 1961). Maidanik (1962) studied the acoustic response of a ribbed panel with a statistical method in the whole frequency range. Results demonstrated that the ribbing increases the radiation resistance of plates. Wallace (1972) investigated mode radiation resistance of a finite rectangular panel using the total radiated energy. Gradually increment and waviness of the radiation resistance were observed below the critical frequency, and solutions asymptotic to unit were obtained after that frequency range. Williams (1983) used a numerical method based on the fast Fourier transform (FFT) to evaluate the velocity response and radiated acoustic pressure of unbaffled finite thin plates. Rayleigh integral and its inverse were employed in iteration calculations, but this method lacks convergence in low frequency range. Harbold and Burroughs (1993) used non-intrusive velocity measurements based on Rayleigh integral to predict acoustic radiation characters of unbaffled plates. The velocity field was obtained with an iteration process, and an algorithm based on FFT was used to calculate the radiated acoustic pressure. Atalla et al. (1996) proposed an analytical formulation to study the acoustic radiation characters of finite thin structures with general elastic boundary conditions. Experiments were also carried out to test the validity of the theoretical approach. Results pointed out that baffles could influence the acoustic radiation obviously in low frequency range. Xie et al. (2005) investigated the average radiation efficiency of plates and stripes with different length-width ratios. The work presented that the acoustic radiation efficiency is proportional to the square of the length of the shorter edge below the fundamental frequency.

On account of the combined environment during service periods of vehicles, structural behaviors influenced by the thermal environment should be considered simultaneously. Jeyaraj et al. (2008) employed the combined approach of finite element and boundary element method (FEM-BEM) to study the vibration and acoustic radiation response of isotropic plates with different boundary conditions in thermal environments. They found that natural frequencies decrease with the increment of plate temperature while the first resonant amplitudes of vibration and sound radiation increase. They also investigated the vibration and acoustic responses of composite plates in thermal environments with the same method (Jeyaraj et al., 2009). A decrement of the resonant amplitude was observed due to damping effects. This variation trend is opposite to the result presented by the previous study. Kumar et al. (2009) carried out parametric studies on vibro-acoustic characteristics of functionally graded material (FGM) elliptic discs in thermal environments with combined FEM and BEM approach. The work presented that vibration responses increase suddenly when the thermal load increases from 0.25 to 0.5 times as the critical buckling temperature. Besides the reported numerical simulations, analytical studies have been conducted on this topic as well. Geng and Li (2012) carried out analytical investigations of the dynamic and acoustic responses of a simply supported rectangular plate in thermal environments. Numerical simulations were used for validation. The analyses were based on the governing equation of vibration with considering the influence of thermally induced membrane forces. Results demonstrated the same variation tendency of natural vibrations with Jeyaraj et al. (2008). It was also found that the first natural frequency seems to be quite sensitive to temperature changes. Acoustic responses indicated that thermal loads have opposite effects on the radiation efficiency of the plate in the frequency ranges below and above the critical frequency. Analytical solutions showed good agreements with numerical results. Response characters of thermally loaded rectangular sandwich plates with simply supported boundaries were also investigated theoretically and numerically (Liu and Li, 2013). Equivalent non-classical theory, which considered the shear and rotational inertia, was used in the work. The influence of variations in structure composition and material properties was discussed as well. In practical engineering applications, clamped boundaries are much more common. So it is necessary to carry out some fundamental studies on it.

The present work has conducted analyses of the dynamic and acoustic radiation characters of a clamped rectangular plate in thermal environments. The general form of governing equation of flexural vibration with considering static thermal loads is established and solved for a clamped plate with uniform temperature changes. Finite element and boundary element (FE-BE) simulations are also employed as validation.

2. Governing equation

Consider a rectangular thin plate vibrating in air fully clamped on all edges, illustrated in Figure 1. The plate is lying in the plane $z = 0$ with dimensions a and b in the two in-plane directions, and h in the thickness. The adjacent acoustic medium occupies the half infinite space $z > 0$. Thermal environment changes will cause temperature variations on the plate, which might induce thermal forces.

This work focuses on the influence of steady thermal distribution on the response characteristics of plates. It is assumed that the temperature remains unchanged during the dynamic process and the stresses caused by thermal loads keep constant as well. The stress state on the plate can be calculated with the combination of two parts, the static stresses induced by temperature changes and the dynamic stresses caused by vibration.

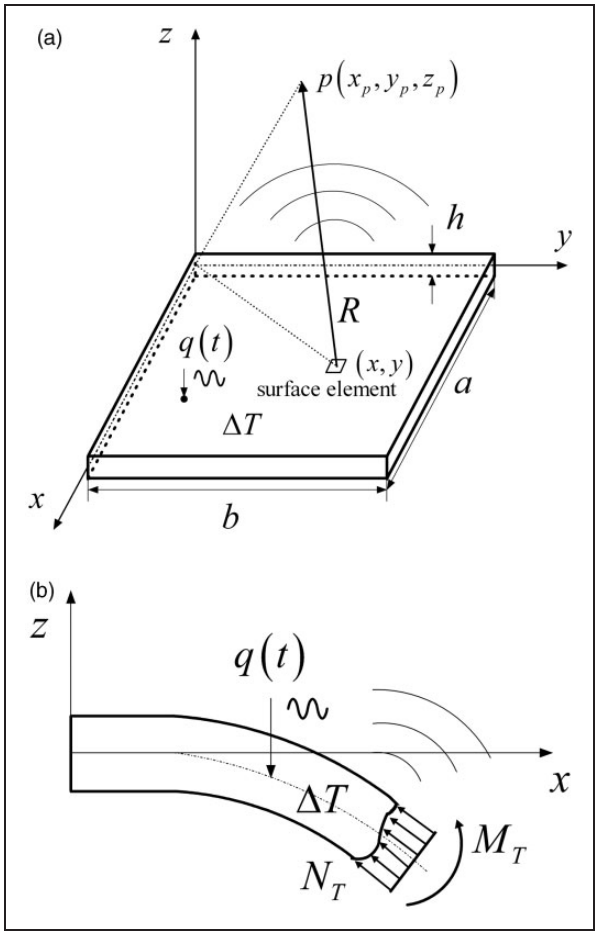

Figure 1. Scratch of the radiating clamped plate: (a) global view, (b) cross section view.

According to the principle of superposition, the stress components of the thermally loaded vibrating plate could be expressed as follows

$$\begin{Bmatrix} \sigma_x \\ \sigma_y \\ \tau_{xy} \end{Bmatrix} = -\frac{Ez}{1-\upsilon^2}\begin{bmatrix} 1 & \upsilon & 0 \\ \upsilon & 1 & 0 \\ 0 & 0 & 1-\upsilon \end{bmatrix}\begin{Bmatrix} \dfrac{\partial^2 w}{\partial x^2} \\ \dfrac{\partial^2 w}{\partial y^2} \\ \dfrac{\partial^2 w}{\partial x \partial y} \end{Bmatrix} + \begin{Bmatrix} \sigma_{Tx}(\Delta T, x, y, z) \\ \sigma_{Ty}(\Delta T, x, y, z) \\ \tau_{Txy}(\Delta T, x, y, z) \end{Bmatrix} \tag{1}$$

where w is the dynamic displacement on the neutral plane of the plate, E is the Young's modulus, υ is the Poisson's ratio, σ_{Tx}, σ_{Ty}, and τ_{Txy} are the thermal stresses, ΔT is the plate temperature change, which is the difference between the current and the original temperature distribution, with positive values denoting temperature rise, and vice versa.

Integrating equation (1) along the plate thickness, one can obtain the expression of the internal forces and moments as

$$\left(\begin{Bmatrix} N_x \\ N_y \\ N_{xy} \end{Bmatrix}, \begin{Bmatrix} M_x \\ M_y \\ M_{xy} \end{Bmatrix}\right) = \left(\int_{-h/2}^{h/2}\begin{Bmatrix} \sigma_{Tx} \\ \sigma_{Ty} \\ \tau_{Txy} \end{Bmatrix} \mathrm{d}z, \begin{Bmatrix} -D\left(\dfrac{\partial^2 w}{\partial x^2} + \upsilon\dfrac{\partial^2 w}{\partial y^2}\right) + \int_{-h/2}^{h/2}\sigma_{Tx}\mathrm{z}\mathrm{d}z \\ -D\left(\dfrac{\partial^2 w}{\partial y^2} + \upsilon\dfrac{\partial^2 w}{\partial x^2}\right) + \int_{-h/2}^{h/2}\sigma_{Ty}\mathrm{z}\mathrm{d}z \\ -D(1-\upsilon)\dfrac{\partial^2 w}{\partial x \partial y} + \int_{-h/2}^{h/2}\tau_{Txy}\mathrm{z}\mathrm{d}z \end{Bmatrix}\right) \tag{2}$$

For an infinitesimal body on the plate, the force balance in the three directions and the moment balance around the x and y axes will be

$$\frac{\partial N_x}{\partial x} + \frac{\partial N_{xy}}{\partial y} = 0 \tag{3}$$

$$\frac{\partial N_{xy}}{\partial x} + \frac{\partial N_y}{\partial y} = 0 \tag{4}$$

$$\frac{\partial Q_x}{\partial x} + \frac{\partial Q_y}{\partial y} + N_x\frac{\partial^2 w}{\partial x^2} + N_y\frac{\partial^2 w}{\partial y^2} + 2N_{xy}\frac{\partial^2 w}{\partial x \partial y} + q - \rho h\frac{\partial^2 w}{\partial t^2} = 0 \tag{5}$$

$$\frac{\partial M_{xy}}{\partial x}+\frac{\partial M_y}{\partial y}-Q_y=0 \tag{6}$$

$$\frac{\partial M_x}{\partial x}+\frac{\partial M_{xy}}{\partial y}-Q_x=0 \tag{7}$$

Substituting equation (2) into equations (3) to (7) and simplifying the expressions, the general form of governing equation of plate flexural vibration with thermal effects can be obtained as

$$\begin{aligned}D_0\nabla^4 w+\rho h\frac{\partial^2 w}{\partial t^2}=q+\int_{-h/2}^{h/2}\sigma_{Tx}\mathrm{d}z\frac{\partial^2 w}{\partial x^2}+\int_{-h/2}^{h/2}\sigma_{Ty}\mathrm{d}z\frac{\partial^2 w}{\partial y^2}\\+2\int_{-h/2}^{h/2}\tau_{Txy}\mathrm{d}z\frac{\partial^2 w}{\partial x\partial y}+\frac{\partial^2}{\partial x^2}\int_{-h/2}^{h/2}\sigma_{Tx}z\mathrm{d}z\\+\frac{\partial^2}{\partial y^2}\int_{-h/2}^{h/2}\sigma_{Ty}z\mathrm{d}z+2\frac{\partial^2}{\partial x\partial y}\int_{-h/2}^{h/2}\tau_{Txy}z\mathrm{d}z\end{aligned} \tag{8}$$

In this work, the influence of uniform temperature changes is studied in detail. In this condition, thermal stresses can be expressed as (Richard and Eslami, 2008)

$$\begin{Bmatrix}\sigma_{Tx}\\ \sigma_{Ty}\\ \tau_{Txy}\end{Bmatrix}=-\frac{E}{1-\upsilon}\begin{Bmatrix}\alpha\Delta T\\ \alpha\Delta T\\ 0\end{Bmatrix} \tag{9}$$

where α is the thermal expansion coefficient.

Substituting equation (9) into equation (8), the governing equation should be

$$D_0\nabla^4 w+\rho h\frac{\partial^2 w}{\partial t^2}=q-\frac{E\alpha\Delta Th}{1-\upsilon}\nabla^2 w \tag{10}$$

where $D_0=Eh^3(1+\mathrm{j}\eta)/12(1-\upsilon^2)$ is the flexural rigidity of the plate, η is the material loss factor taking damping effects into account (Pritz, 1998), j is the imaginary unit, ρ is the mass density, q is the applied excitation.

3. Natural vibration

3.1. Approximate solution

Natural frequencies and mode shapes of the thermally loaded plates are studied at first. Omitting the excitation term on the right side of equation (10), free vibration of plates under static thermal loads can be obtained as

$$D_0\nabla^4 w+\frac{E\alpha\Delta Th}{1-\upsilon}\nabla^2 w+\rho h\frac{\partial^2 w}{\partial t^2}=0 \tag{11}$$

The solution of equation (11) can be expressed as the sum of principal vibrations

$$w(x,y,t)=\sum_{m,n}w_{mn}\phi_{mn}(x,y)e^{\mathrm{j}\omega t} \tag{12}$$

where w_{mn} is the modal displacement amplitude of the mode (m,n), and $\phi_{mn}(x,y)$ is the corresponding mode shape function, ω is the response frequency.

For the fully clamped boundary condition, mode shape functions should satisfy the requirement of zero translations and zero rotations on all edges of the plate. Mode shape expressions with cosine components as (Murphy et al., 1997)

$$\begin{aligned}\phi_{mn}(x,y)=&\left(\cos\frac{(m-1)\pi x}{a}-\cos\frac{(m+1)\pi x}{a}\right)\\&\times\left(\cos\frac{(n-1)\pi y}{b}-\cos\frac{(n+1)\pi y}{b}\right)\end{aligned} \tag{13}$$

and as (Xin and Lu, 2009; Sha et al., 2012)

$$\phi_{mn}(x,y)=\left(1-\cos\frac{2m\pi x}{a}\right)\times\left(1-\cos\frac{2n\pi y}{b}\right) \tag{14}$$

are used in previous studies. There is also a set of shape functions with sinusoidal components for clamped plates as follows (Cao, 1989)

$$\begin{aligned}\phi_{mn}(x,y)=&\left[(-1)^m\left(\frac{x^3}{a^3}-\frac{x^2}{a^2}\right)+\left(\frac{x^3}{a^3}-2\frac{x^2}{a^2}+\frac{x}{a}\right)-\frac{1}{m\pi}\sin\frac{m\pi x}{a}\right]\\&\times\left[(-1)^n\left(\frac{y^3}{b^3}-\frac{y^2}{b^2}\right)+\left(\frac{y^3}{b^3}-2\frac{y^2}{b^2}+\frac{y}{b}\right)-\frac{1}{n\pi}\sin\frac{n\pi y}{b}\right]\end{aligned} \tag{15}$$

Although the expression of equation (15) is much more complicated, natural frequencies obtained with sinusoidal mode shape functions are closer to finite element solutions, especially for high order modes, than the results obtained with equations (13) and (14) using the same number of mode terms. This has been confirmed in preliminary work. Therefore, the last mode shape function set is selected in this study.

Substituting equations (12) and (15) into equation (11), it can be expanded as the form of double Fourier series

$$\begin{aligned}L(w)&=D_0\nabla^4 w+\frac{E\alpha\Delta Th}{1-\upsilon}\nabla^2 w+\rho h\frac{\partial^2 w}{\partial t^2}\\&=\sum_{m,n}\beta_{mn}\sin\frac{m\pi x}{a}\sin\frac{n\pi y}{b}=0\end{aligned} \tag{16}$$

β_{mn} is the Fourier coefficient which should satisfy the following condition

$$\beta_{mn} = \frac{4}{ab}\iint_S L(w)\sin\frac{m\pi x}{a}\sin\frac{n\pi y}{b}\mathrm{d}A = 0 \qquad (17)$$

A homogenous system of linear equations in the unknown mode amplitudes w_{mn} can be established with equation (17) as

$$[\mathbf{C}]_{(M\times N)\times(M\times N)}\{w_{mn}\}_{(M\times N)} = \{0\}_{(M\times N)} \qquad (18)$$

where $[\mathbf{C}]$ is the coefficient matrix with elements generated during the process of integration, $M \times N$ is the number of mode terms used in the analysis. Because the shape functions used here are not orthogonal with respect to the inner product, the coefficient matrix is actually full. To guarantee the existence of nonzero solution sets for equation (18), the determinant of the coefficient matrix must be zero. Therefore, a polynomial equation in the unknown frequency of degree $2M \times N$ will be founded, and the roots are the natural frequencies of the plate.

According to Abel-Ruffini theorem, closed-form solutions cannot be found for polynomial equations of degrees higher than four. In practical analyses, the number of concerned natural frequencies is often much greater than that value. Numerical methods with iterative processes are needed to solve the equation. There might be problems in numerical stability. On the other hand, it is also hard to determine the mode shapes related to the calculated natural frequencies.

In forced vibration problems, the dynamic response of structures will increases rapidly when the excitation frequency is getting close to any natural frequency, and the related principle vibration plays the dominating role. For undamped structures, the mode amplitude of the corresponding mode goes to infinite as resonance occurs. Therefore, the natural frequencies of the heated clamped plate can be approximately evaluated by searching the null points of the reciprocals of mode amplitudes. According to the solution formula, this method is also feasible for simply supported plate (Geng and Li, 2012). The solving procedure is implemented as follows.

a. Obtain the Fourier series expansion of the forced vibration equation of plates under thermal loads with equations (10), (12), and (15)

$$\begin{aligned} L'(w) &= D_0\nabla^4 w + \frac{E\alpha\Delta Th}{1-\upsilon}\nabla^2 w + \rho h\frac{\partial^2 w}{\partial t^2} - q \\ &= \sum_{m,n}\beta'_{mn}\sin\frac{m\pi x}{a}\sin\frac{n\pi y}{b} = 0 \end{aligned} \qquad (19)$$

where the Fourier coefficient β'_{mn} should satisfy the following requirement

$$\beta'_{mn} = \frac{4}{ab}\iint_S L'(w)\sin\frac{m\pi x}{a}\sin\frac{n\pi y}{b}\mathrm{d}A = 0 \qquad (20)$$

b. With equation (20), a nonhomogeneous system of linear equations in the unknown mode amplitudes of forced vibration can be founded as

$$[\mathbf{C}]'_{(M\times N)\times(M\times N)}\{w_{mn}\}'_{(M\times N)} = \{\mathbf{Q}\}_{(M\times N)} \qquad (21)$$

where $\{\mathbf{Q}\}$ is the excitation vector.

c. Solve the linear system and obtain the expressions for the mode amplitudes.
d. Solve the null points of the reciprocals of the mode amplitudes, and the solutions are the natural frequencies corresponding to the relevant modes.

With this method, the natural frequencies are calculated with $M \times N$ polynomial equations, which are obtained with the reciprocals of mode amplitudes. The degrees of the polynomial equations in frequency are generally no more than four. The computational burden increases linearly with the number of the used mode terms. With the previous method, conducted with free vibrations, one polynomial equation of degree $2M \times N$ needs to be solved. The computational effort increases much faster than the method conducted with forced vibrations, in the meanwhile, the numerical stability decreases obviously. Therefore, the second method described in this section is used in this work for its brevity and stability.

3.2. Case study

A clamped rectangular aluminum plate with length 0.3 m, width 0.2 m, and thickness 0.003 m is studied in detail. The material properties are Young's modulus 65 GPa, Poisson's ratio 0.27, mass density 2810 $\mathrm{kg\,m^{-3}}$, loss factor 0.001, and thermal expansion coefficient $2.3\times10^{-5}\,\mathrm{K^{-1}}$. The material properties of the plate are considered to be temperature independent.

At first, a convergence analysis is carried out for the natural frequencies of the clamped plate without thermal loads, shown in Table 1. According to the results, six is selected for both M and N in this calculation.

For constrained plates, thermal buckling will occur as the temperature change is large enough. And the thermal load is called the critical buckling temperature T_c. In this condition, the equilibrium configuration of the plate will not be flat anymore, and the solutions

Table 1. Convergence analysis for the natural frequencies of the clamped plate (Hz).

$M \times N$	$(m=1, n=1)$	$(m=2, n=1)$	$(m=1, n=2)$	$(m=3, n=1)$	$(m=2, n=2)$
4×4	462.0	711.1	1134.7	1145.3	1360.3
5×5	463.8	713.5	1136.5	1140.5	1360.3
6×6	463.8	715.0	1136.2	1140.5	1367.1
7×7	464.3	715.8	1137.0	1142.3	1367.1

Table 2. Approximate results of natural frequencies in different thermal environments (Hz).

Thermal loads	$(m=1, n=1)$	$(m=2, n=1)$	$(m=1, n=2)$	$(m=3, n=1)$	$(m=2, n=2)$
0°C	463.8	715.0	1136.2	1140.5	1367.1
10°C	367.4	604.4	1029.1	1026.2	1254.8
20°C	229.4	465.6	908.3	896.3	1130.3
26.1°C	28.7	353.2	825.2	806.2	1046.6

given in this work will not be suitable. Therefore, thermal loads are all designed below the critical buckling temperature of the plate in the calculations. The critical buckling load of plates with in-plane loads can be obtained by solving the static governing equation as (Timoshenko and Gere, 1985)

$$D_0 \nabla^4 w = N_x \frac{\partial^2 w}{\partial x^2} + N_y \frac{\partial^2 w}{\partial y^2} + 2N_{xy} \frac{\partial^2 w}{\partial x \partial y} \qquad (22)$$

Substituting equations (2), (9), and (15) into equation (22), and applying the mode shape function with $(m = 1, n = 1)$, the first order critical buckling temperature can be evaluated.

The tedious process for solving equation (22) is omitted for simplicity, and the critical buckling temperature for the plate model described above is about 26.2°C as calculated. Therefore, two thermal load cases with temperature rises of 10 and 20°C are chosen. Structural temperature of 0°C is defined as the reference case to represent the stress free state. A thermal load case with temperature rise of 26.1°C, which is quite close to the critical buckling temperature, is also selected.

The approximate solutions of the first five natural frequencies of the clamped plate under different thermal loads are listed in Table 2. Results show that the frequencies decrease evidently with the increment of temperature. Meanwhile, the natural frequency of mode (3, 1) becomes lower than the value of mode (1, 2) when the plate temperature is elevated. For these two modes, the natural frequencies are quite close to each other with relative errors no more than 2.5% in all the concerned thermal conditions. This phenomenon of mode shape interchange is not observed for the heated simply supported plate presented by Geng and Li (2012).

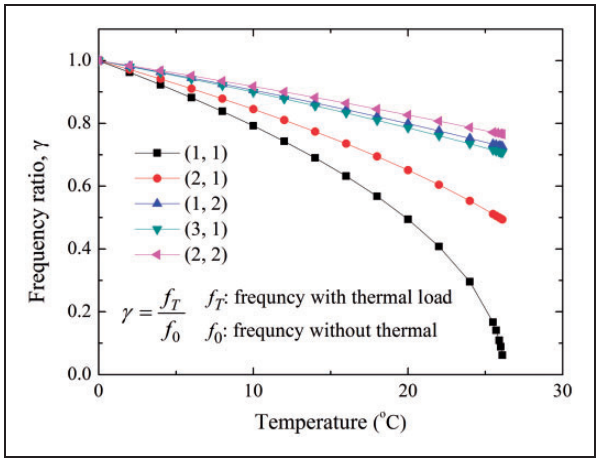

Figure 2. Frequency ratios versus plate temperature.

Frequency ratios, defined by f_T/f_0, versus the structural temperature are plotted in Figure 2. f_T and f_0 are the natural frequencies obtained with thermal loads and in the reference environment (0°C in this work), respectively. The curves are depicted with dense data points to describe the variation tendency near the buckling point. It is obvious that the first natural frequency is much more sensitive to the temperature changes than other frequencies. It can be seen from the curves that when the structural temperature is quite close to the critical buckling temperature, the first frequency ratio reduces to almost zero, and the slope of the curve goes to negative infinity.

Table 3. Convergence analysis for the natural frequencies of the FE plate model (Hz).

Mesh density	$(m=1, n=1)$	$(m=2, n=1)$	$(m=1, n=2)$	$(m=3, n=1)$	$(m=2, n=2)$
30×20	462.3	710.5	1129.8	1131.3	1351.9
45×30	463.2	713.6	1132.1	1136.6	1360.4
60×40	463.5	714.7	1132.9	1138.5	1363.6
75×50	463.7	715.2	1133.3	1139.5	1365.1

Table 4. Errors of natural frequencies between the approximate and FE solutions (%).

Thermal loads	$(m=1, n=1)$	$(m=2, n=1)$	$(m=1, n=2)$	$(m=3, n=1)$	$(m=2, n=2)$
0°C	−0.05	−0.05	−0.29	−0.18	−0.26
10°C	−0.32	−0.29	−0.44	−0.51	−0.40
20°C	−1.17	−0.75	0.64	−1.02	−0.59

Finite element simulations are employed for validation studies. In the finite element formulation, pre-stressed modal analyses with membrane forces can be carried out with considering the stress stiffness as (Robert et al., 1989)

$$\left([\mathbf{K}+\mathbf{K}_\sigma]-\omega^2[\mathbf{M}]\right)\{\mathbf{U}\}=\{0\} \tag{23}$$

where $[\mathbf{K}]$ is the conventional stiffness matrix, $[\mathbf{M}]$ is the mass matrix, ω is the angular frequency, $\{\mathbf{U}\}$ is the amplitude vector of nodal degree of freedom (DOF), $[\mathbf{K}_\sigma]$ is the stress stiffness matrix which can be defined for plate model as

$$[\mathbf{K}_\sigma]=\sum_i \int_{A_i} [\mathbf{G}]^{\mathrm{T}} \begin{bmatrix} N_x & N_{xy} \\ N_{xy} & N_y \end{bmatrix} [\mathbf{G}] \mathrm{d}A \tag{24}$$

where $[\mathbf{G}]$ is the strain-displacement matrix, A_i is the area of the ith element.

In this work, the membrane forces are induced by plate temperature changes, and can be obtained by static thermo-elastic analysis. Then, the modal parameters of the thermally loaded plates could be calculated via pre-stressed modal analyses.

The FEM software package MD Nastran is employed to carry out the simulations. The plate is modeled with four-node quadrilateral plate elements (CQUAD4). All the six DOFs of nodes on the plate edges are constrained to implement clamped boundary conditions. Linear static solver (sol 101) is selected to conduct thermo-elastic analyses at first. And then, the calculated thermal stresses are used as pre-stresses in normal mode predictions with normal mode solver (sol 103). A convergence study is also conducted for the FE model without thermal effects, as shown in Table 3. Based on the results, the mesh density of 60×40 is selected.

Errors between the approximate results and FE solutions relative to the former ones are illustrated in Table 4. It is clear that natural frequencies obtained with the approximate approach compare well with the ones obtained with FEM in the three thermal conditions. The errors indicate that approximate solutions are generally higher. And the errors rise slightly when considering the influence of thermal loads. However, the maximum value is no more than 1.2%. Same relationships can also be observed for higher order natural frequencies for both the cases with and without thermal effects. Results obtained with FEM also present the mode shape interchange between mode (3, 1) and mode (1, 2).

In the FE simulation for the case with 26.1°C temperature change, the first natural vibration disappears. It means that the applied thermal load has already exceeded the critical buckling temperature, which is about 26°C obtained with MD Nastran, for the FE model. It is known from Figure 2 that the variation ratio for the first natural frequency is extremely high near the critical buckling temperature. The frequency value is quite sensitive to the temperature change. The error for the first natural frequency rises rapidly in a small temperature range because of the sensitivity of the frequency to temperature.

4. Dynamic response

4.1. Approximate solution

In the previous section, the mode amplitudes of forced vibration have already been obtained during the procedure for solving natural frequencies with the approximate method. Therefore, the displacement response of the plate can be calculated with equation (12), velocity and acceleration responses can be obtained as well.

Accordingly, acoustic radiation characters in the far field of the vibrating plate could be evaluated by Rayleigh integral (Fahy and Gardonio, 2007)

$$p(x_p, y_p, z_p, t) = \frac{j\omega\rho_a}{2\pi} e^{j\omega t} \int_{\Omega} \frac{\sum_{m,n} v_{mn}\phi_{mn}(x,y) \cdot e^{-jkR}}{R} dA \tag{25}$$

where v_{mn} is the modal velocity amplitude of mode (m,n), ρ_a is the air density, R is the distance between the observation point (x_p, y_p, z_p) and the integration point on the plate, k is the wave number evaluated by the vibration frequency ω and the speed of sound c_0 with $k = \omega/c_0$. Based on the radiated acoustic pressure, other parameters, such as sound radiation power and radiation efficiency, can be calculated to investigate the acoustic radiation characters further.

A transverse harmonic concentrated excitation with unit amplitude is applied on the plate to investigate the response characters. The excitation point is selected in the location with quarter of the length and the width to avoid the nodal lines of the first five modes. The structural vibration and acoustic radiation responses are studied in the frequency range below 2000 Hz. Physical properties of the acoustic medium are density $1.21\,\mathrm{kg\,m^{-3}}$, and the speed of sound $343\,\mathrm{m\,s^{-1}}$. The temperature of the acoustic domain is assumed constant in this analysis.

The displacement and velocity responses on the center of the plate are plotted in Figure 3 and Figure 4, respectively. It is clear that the dynamic responses of the plate shift toward lower frequency range integrally with the increment of temperature. The global characters of the responses stay the same in different environments. This variation tendency is mainly determined by the variation in natural vibrations in thermal environments. Comparing the responses at the first resonance peak, it can be seen that the response amplitude of displacement stays almost unchanged until a sudden increment occurs when the temperature rises to 26.1°C. The resonant amplitude of velocity shows oscillation with temperature changes.

When the constrained plate is heated, compressive forces act in the structure. The softening effect induced by thermal loads will make the response amplitude of displacement higher. In the meanwhile, the first resonant peak appears at lower frequency point when the plate temperature is elevated. For steady state, the velocity response can be obtained by multiplying the displacement by the response frequency. The above two variations make the resonant amplitude of velocity oscillates in thermal environments.

Acoustic radiation of the clamped plate in different thermal environments is calculated, and the sound

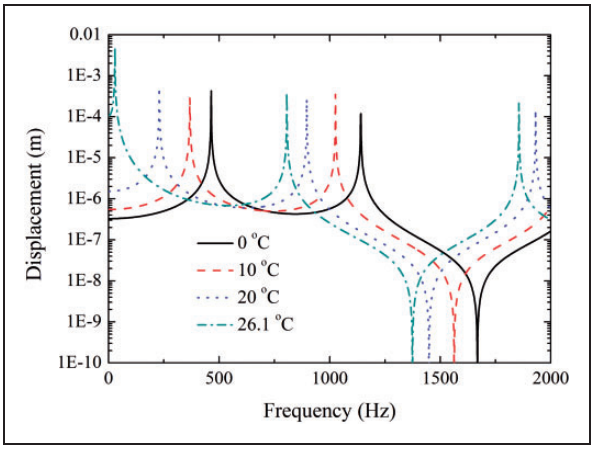

Figure 3. Displacement response on the center of the clamped plate.

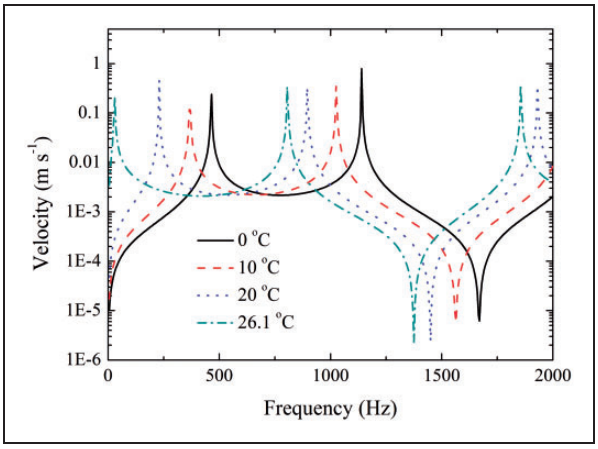

Figure 4. Velocity response on the center of the clamped plate.

radiation power level of the heated plate versus the excitation frequency is plotted in Figure 5. Been affected by the vibration response directly, the radiation power response shifts toward lower frequency range as well, with the global characters unchanged. On the contrary, the first resonant amplitude decreases obviously in thermal environments, which is not in agreement with the variation tendency of plate vibration response. This phenomenon is mainly caused by the variation in the first resonant frequency. It can be known from Rayleigh integral that the radiated acoustic pressure is proportional to both the velocity response and the vibration frequency. When the plate is heated, the velocity response amplitude almost stays the same at the first resonant peak (see Figure 4). Meanwhile, the resonant peak shifts toward lower frequency range. This combined effect leads to the decrement of the radiated acoustic pressure, and then a reduction of the sound radiation power level appears.

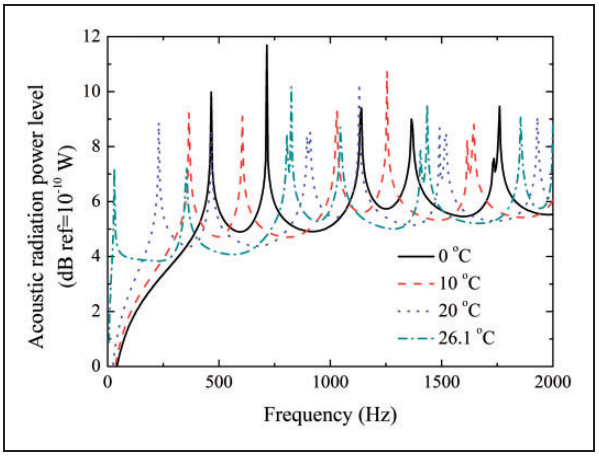

Figure 5. Sound radiation power level of the clamped plate.

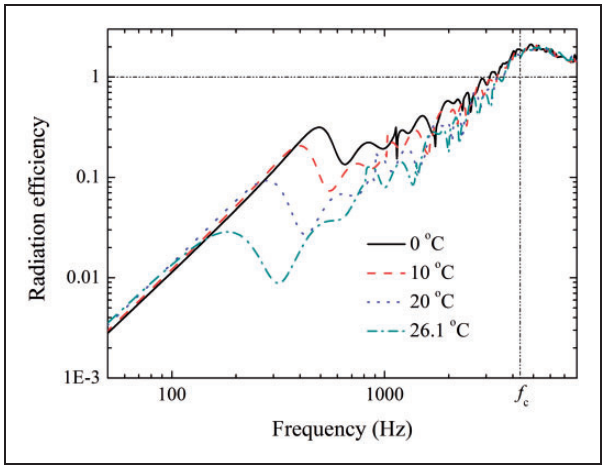

Figure 6. Acoustic radiation efficiency of the clamped plate in thermal environments.

Radiation efficiency is a parameter to describe the radiating effectiveness of vibrating structures. It is obtained by dividing the radiation power with acoustic impedance, structure area and the vibrating velocity on the surface (Fahy and Gardonio, 2007). Figure 6 gives the radiation efficiency of the clamped plate with different thermal loads. Compared well with Wallace (1972), the efficiency shows gradual increment and waviness below the critical frequency f_c, about 4330 Hz for this plate. In higher frequency range, the radiation efficiency reduces to unit asymptotically.

When the plate is heated, the radiation efficiency decreases obviously in the frequency range above about 150 Hz. The first wave comes earlier and the peak value reduces about 90% of the initial value, without thermal effects, as the plate temperature is quite close to the critical buckling temperature. With the increment of frequency, the influence of thermal loads becomes weaker. The maximum radiation efficiency

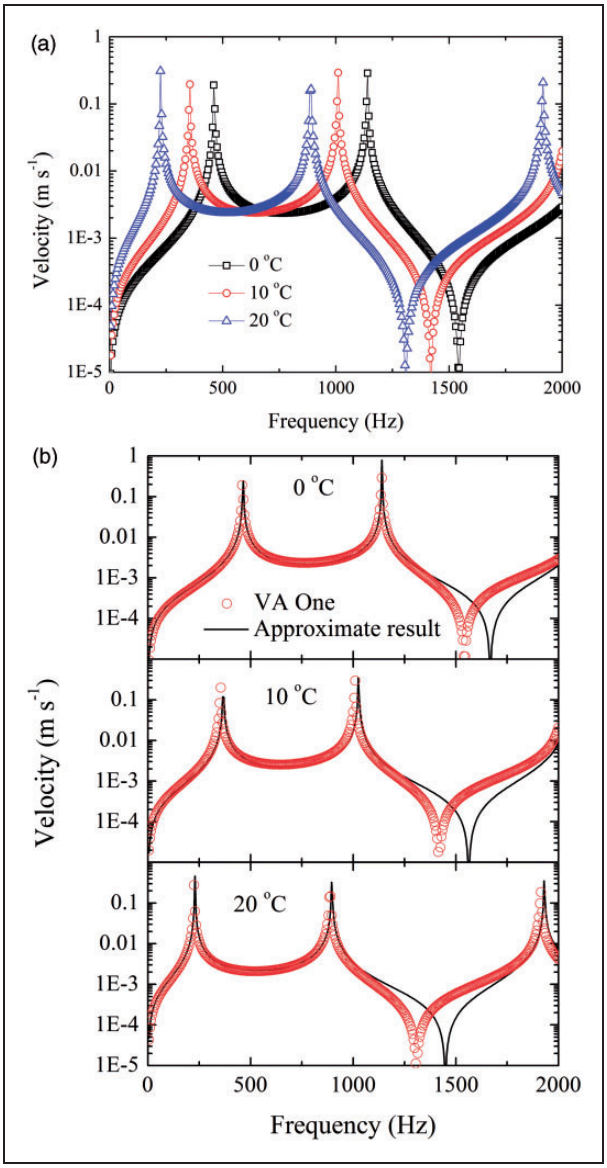

Figure 7. Simulated velocity responses and comparisons with approximate results: (a) FE solutions from VA One, (b) velocity comparisons between approximate and simulated results.

value almost stays the same in different thermal environments. It is clear that the radiation efficiency in the frequency range below 150 Hz rises slightly in thermal environments. A slight decrement can be observed in the frequency range above the critical frequency.

4.2. FE-BE simulation

The response characters are also studied with simulations. The software package VA One with combined FEM and BEM approach is employed. The FE plate model is borrowed from the previous modal analyses, and the acoustic medium is modeled with a semi-infinite BEM fluid. Natural frequencies and mode shapes are

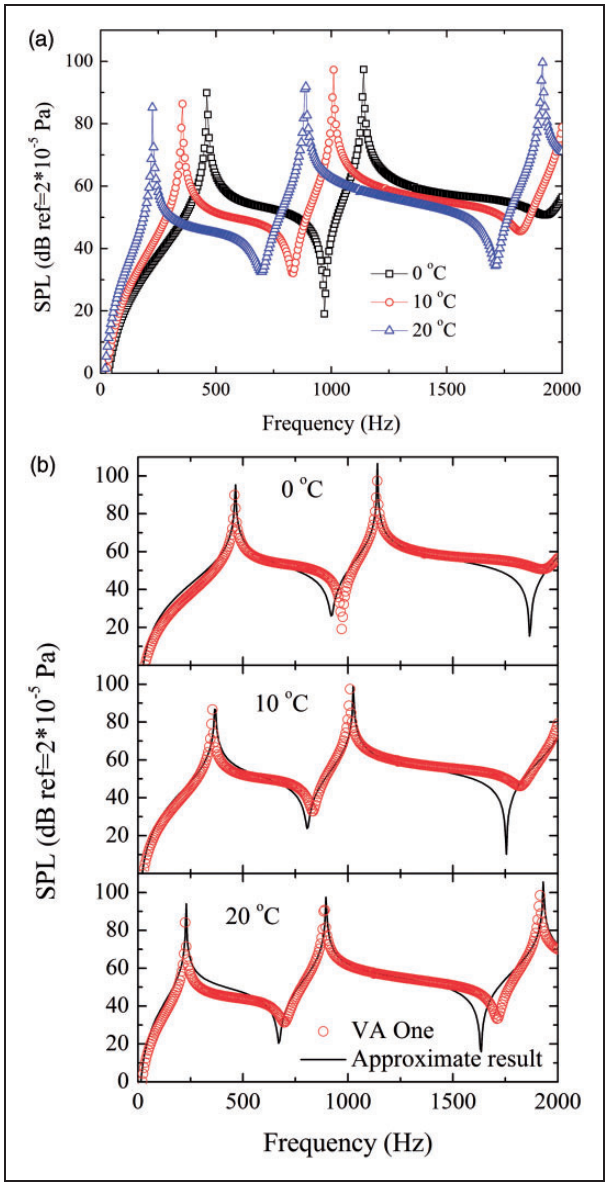

Figure 8. Simulated SPL responses and comparisons with approximate results: (a) FE-BE solutions from VA One, (b) SPL comparisons between approximate and simulated results.

imported into VA One from Nastran result files obtained from the normal mode analyses presented in Section 3. The structural response is calculated with FEM solver, and the acoustic radiation response is obtained with BEM solver.

FE results of velocity responses and comparisons with approximate solutions at the centroid point on the plate are shown in Figure 7. It appears that FE results show same variation tendency of velocity in thermal environments with the approximate solutions. The response curve shifts toward lower frequency range, and the first resonant amplitude increases slightly with the increment of temperature. The response curves compare well, while a mismatch can be observed at the antiresonance frequency.

The sound pressure level (SPL) responses are predicted at the point in the acoustic medium located 2 m above the center of the plate with FE-BE simulations, and also compared with the results obtained with the approximate approach, plotted in Figure 8. The same as the approximate results, the simulated SPL response amplitude shows an opposite variation trend at the first resonant peak in thermal environments. Influenced by the velocity response, the errors of SPL responses between the approximate and FE-BE results become more obvious at antiresonance points as well.

5. Conclusions

This work presents the study of the influence of thermal effects on dynamic and acoustic radiation characteristics of a clamped rectangular plate, and numerical simulations are also employed as validations. Thermal stresses, induced by thermal variations, are treated as static initial stresses and taken into account in the equilibrium condition of the infinitesimal body of the plate. The general form of governing equation of plate flexural vibration with considering static thermal loads is established, and the response characters of a clamped rectangular plate with uniform temperature changes are analyzed in detail.

The approximate results indicate that natural frequencies of plate decrease with the increment of temperature. Mode shape interchange occurs for the modes with close natural frequencies. Approximate solutions match well with the FE ones. The first natural frequency is much more sensitive to thermal environment changes. When the structural temperature is quite close to the critical buckling value, the errors between the approximate and simulated results get lager rapidly in a small temperature range close to the critical buckling temperature.

The responses of plate vibration and sound radiation power shift toward lower frequency range in thermal environments, and the global characters of responses stay the same. The first resonant amplitude of displacement increases obviously when the plate temperature approaches the critical buckling value, and the sound radiation power decreases gradually. With thermal effects, the radiation efficiency of the clamped plate reduces obviously before the critical frequency. FE-BE solutions compare well with the approximate solutions except the values at antiresonance points.

Funding

This work is supported by the National Natural Science Foundation of China (grant numbers 11321062, 91016008, and 91216107).

References

Atalla N, Nicolas J and Gauthier C (1996) Acoustic radiation of an unbaffled vibrating plate with general elastic boundary conditions. *Journal of the Acoustical Society of America* 99: 1484–1494.

Behrens B and Muller M (2004) Technologies for thermal protection systems applied on re-usable launcher. *Acta Astronautica* 55: 529–536.

Boley BA (1956) Thermally induced vibration of beams. *Journal of the Aeronautical Sciences* 23: 179–181.

Boley BA and Barber AD (1957) Dynamic response of beams and plates. *Journal of Applied Mechanics Trans ASME* 24: 413–416.

Cao ZY (1989) *Vibration Theory of Plates and Shells (in Chinese)*. Beijing: China Railway Press.

David CG (1961) Vibration and sound radiation of damped and undamped flat plates. *Journal of the Acoustical Society of America* 33: 1315–1320.

Fahy F and Gardonio P (2007) *Sound and Structural Vibration: Radiation, Transmission and Response (Second Edition)*. Boston: Academic Press.

Ganesan N and Dhotarad MS (1984) Hybrid method for analysis of thermally stressed plates. *Journal of Sound and Vibration* 94: 313–316.

Geng Q and Li Y (2012) Analysis of dynamic and acoustic radiation characters for a flat plate under thermal environments. *International Journal of Applied Mechanics* 4: 1250028.

George C (1961) Sound radiation from prolate spheroids. *Journal of the Acoustical Society of America* 33: 871–876.

Harbold TL and Burroughs CB (1993) Numerical predictions of acoustic radiation by unbaffled finite plates from non-intrusive velocity. *Journal of the Acoustical Society of America* 93: 2389–2389.

Jadeja ND and Loo TC (1974) Heat induced vibration of a rectangular plate. *Journal of Engineering for Industry* 96: 1015–1021.

Jeyaraj P, Ganesan N and Padmanabhan C (2009) Vibration and acoustic response of a composite plate with inherent material damping in a thermal environment. *Journal of Sound and Vibration* 320: 322–338.

Jeyaraj P, Padmanabhan C and Ganesan N (2008) Vibration and acoustic response of an isotropic plate in a thermal environment. *Journal of Vibration and Acoustics Trans ASME* 130: 70510055.

Kim YW (2005) Temperature dependent vibration analysis of functionally graded rectangular plates. *Journal of Sound and Vibration* 284: 531–549.

Kumar BR, Ganesan N and Sethuraman R (2009) Vibro-acoustic analysis of functionally graded elliptic disc under thermal environment. *Mechanics of Advanced Materials and Structures* 16: 160–172.

Liu Y and Li Y (2013) Vibration and acoustic response of rectangular sandwich plate under thermal environment. *Shock and Vibration* 20: 1011–1030.

Maidanik G (1962) Response of ribbed panels to reverberant acoustic fields. *Journal of the Acoustical Society of America* 34: 809–826.

Murphy KD, Virgin LN and Rizzi SA (1997) The effect of thermal prestress on the free vibration characteristics of clamped rectangular plates: theory and experiment. *Journal of Vibration and Acoustics Trans ASME* 119: 243–249.

Pritz T (1998) Frequency Dependences of complex moduli and complex poisson's ratio of real solid materials. *Journal of Sound and Vibration* 214: 83–104.

Richard BH and Eslami MR (2008) *Thermal Stresses-Advanced Theory and Applications*. Netherlands: Springer.

Robert C, David M and Michael P (1989) *Concepts and Application of Finite Element Analysis (Third Edition)*. New York: John Willy & Sons.

Sha YD, Wei jJ, Gao ZJ and Zhong HJ (2012) Nonlinear response with snap-through and fatigue life prediction for panels to thermo-acoustic loadings. *Journal of Vibration and Control* 20: 679–697.

Timoshenko SP and Gere JM (1985) *Theory of Elastic Stability*. New York: McGraw-Hill Book Company Inc.

Wallace CE (1972) Radiation resistance of a rectangular panel. *Journal of the Acoustical Society of America* 51: 946–952.

Wilby JF (1996) Aircraft interior noise. *Journal of Sound and Vibration* 190: 545–564.

Williams EG (1983) Numerical evaluation of the radiation from unbaffled, finite plates using the FFT. *Journal of the Acoustical Society of America* 74: 343–347.

Xie G, Thompson DJ and Jones CJC (2005) The Radiation efficiency of baffled plates and strips. *Journal of Sound and Vibration* 280: 181–209.

Xin FX and Lu TJ (2009) Analytical and experimental investigation on transmission loss of clamped double panels: implication of boundary effect. *Journal of the Acoustical Society of America* 125: 1506–1517.

Yeh YL (2005) The effect of thermo-mechanical coupling for a simply supported orthotropic rectangular plate on nonlinear dynamics. *Thin-Walled Structure* 43: 1277–1295.